

# Probing the mRNA processing body using protein macroarrays and “autoantigenomics”

WEI-HONG YANG and DONALD B. BLOCH

Center for Immunology and Inflammatory Diseases of the General Medical Services, Massachusetts General Hospital and Harvard Medical School, Boston, Massachusetts 02129, USA

## ABSTRACT

Messenger RNA processing bodies (P-bodies) are cellular structures that have a direct role in mRNA degradation. P-bodies have also been implicated in RNAi-mediated post-transcriptional gene silencing. Despite the important roles of P-bodies in cellular biology, the constituents of P-bodies and their organization have been only partially defined. Approximately 5% of patients with the autoimmune disease primary biliary cirrhosis have antibodies directed against these structures. Recent advances in protein macroarray technology permit the simultaneous screening of thousands of proteins for reactivity with autoantibodies. We used serum from patients with anti-P-body autoantibodies to screen a protein macroarray and identified 67 potential autoantigens. Immunoreactive proteins included four known P-body components and three additional primary biliary cirrhosis autoantigens. Y-box protein 1 (YB-1), a 50-kDa RNA-binding protein that was not previously known to be a P-body component, was recognized by serum from four of seven patients. YB-1 colocalized with P-body components DCP1a and Ge-1. In cells subjected to arsenite-induced oxidative stress, YB-1 localized to TIA-containing stress granules. Both YB-1 and the previously identified P-body component RAP55 translocated from P-bodies to stress granules during oxidative stress. During recovery, however, the reappearance of YB-1 in P-bodies was delayed compared with that of RAP55, suggesting that YB-1 and RAP55 may have different functions. This study demonstrates that the combination of human autoantibodies and protein macroarray technology provides a novel method for identifying and characterizing components of mRNA P-bodies.

**Keywords:** mRNA processing body; stress granule; mRNA decay; autoantigen; protein macroarray

## INTRODUCTION

Messenger RNA storage and degradation are critical steps in the regulation of gene expression. Cytoplasmic mRNA processing bodies (P-bodies, also known as “cytoplasmic foci” and GW182 bodies) are multiprotein complexes that have a central role in the regulation of mRNA metabolism (Eystathioy et al. 2003; Sheth and Parker 2003; Cougot et al. 2004). P-bodies contain decapping enzymes (DCP1a and DCP2) that remove the 5' cap of mRNA and a 5' to 3' exoribonuclease (Xrn1). These structures also contain seven “Sm-like” proteins (LSm1–7), which form a heptameric complex that binds mRNA, and the DEAD box family helicase Rck/p54, which increases the efficiency of mRNA decapping (Bouveret et al. 2000; Coller et al. 2001; Eystathioy et al. 2003; Cougot et al. 2004). Three autoantigens, GW182, Ge-1, and RAP55, also localize to P-bodies

(Eystathioy et al. 2003; Fenger-Gron et al. 2005; Yu et al. 2005; Yang et al. 2006). GW182 recruits Argonaute proteins, key components of the RNA interference machinery, to P-bodies (Jakymiw et al. 2005; Liu et al. 2005). Silencing of GW182 disrupts P-bodies and inhibits translational repression by miRNA, suggesting that there is a functional link between RNAi and P-bodies (Jakymiw et al. 2005; Liu et al. 2005). Ge-1, also known as Hedls, interacts with the core decapping enzymes and enhances mRNA degradation (Fenger-Gron et al. 2005; Yu et al. 2005). The third P-body autoantigen, RAP55, contains an Sm-like domain and two RGG-type RNA-binding motifs. RAP55 localizes to P-bodies and, in response to oxidative stress, translocates to stress granules. RAP55 rapidly returns to P-bodies during the recovery period, suggesting that RAP55 may have a role in shuttling mRNA between stress granules and P-bodies (Yang et al. 2006).

P-bodies have a dynamic relationship with polyribosomes and stress granules (Bregues et al. 2005; Kedersha et al. 2005; Yu et al. 2005). In cells that are treated with cyclohexamide, a translation elongation inhibitor that traps mRNAs in polyosomes, P-bodies rapidly disappear. In contrast, displacement of mRNAs from polysomes by puromycin increases the size

**Reprint requests to:** Donald B. Bloch, Center for Immunology and Inflammatory Diseases of the General Medical Services, Massachusetts General Hospital-East, CNY 8302, 149 13th Street, Charlestown, MA 02129, USA; e-mail: bloch@helix.mgh.harvard.edu; fax: (617) 726-5651.

Article published online ahead of print. Article and publication date are at <http://www.rnajournal.org/cgi/doi/10.1261/rna.411907>.

and number of P-bodies. During environmental stress, translation of mRNAs encoding housekeeping proteins is discontinued, and these mRNAs are stored in stress granules for potential future use (for review, see Kedersha and Anderson 2002). Stress granules contain small ribosome subunits, translation initiation factors, and a variety of RNA-binding proteins. Antibodies directed against TIA, a central component of stress granules, serve as a marker for these structures. The sequestration of housekeeping mRNAs permits mRNAs encoding cellular repair proteins to gain access to the translation machinery. P-bodies and stress granules interact with each other during and after environmental stress, and some P-body components, including RAP55 and Xrn1, are found in both P-bodies and stress granules (for review, see Anderson and Kedersha 2006). During the recovery period, stress granules may serve as a “sorting” domain for mRNAs. A subset of mRNAs may be recycled and returned to polysomes to restart protein synthesis. In contrast, other mRNAs may be transferred to adjacent P-bodies for destruction. The mechanism by which mRNAs are separated, for either reuse or destruction, is unknown.

Primary biliary cirrhosis (PBC) is an autoimmune disease of unknown etiology characterized by the progressive destruction of intrahepatic biliary ductules, leading to hepatic fibrosis and liver failure (for review, see Kaplan and Gershwin 2005). Approximately 5% of PBC patients have antibodies directed against P-bodies (Bloch et al. 2005). Recent advances in the field of proteomics have facilitated the development of a membrane-based macroarray that permits high-throughput screening of human proteins using autoantibodies (Bussow et al. 2000). The technique involves preparation of a cDNA library in a prokaryotic expression vector, transformation of bacteria, and growth of individual clones in microtiter wells. The bacteria are robotically transferred, at high density, to nitrocellulose membranes and are induced to express the cDNA in situ. This technique was used by other investigators to identify the targets of autoantibodies in patients with cardiac and dermatologic disorders (Lueking et al. 2005; Horn et al. 2006). In the present study, we used serum from patients with primary biliary cirrhosis and protein macroarray technology to identify potential P-body autoantigens and show that Y-box protein 1 (YB-1) is a novel component of these structures.

## RESULTS AND DISCUSSION

### PBC autoantibodies react with proteins in a macroarray

Using indirect immunofluorescence and the Hep-2 cell line as a substrate, 34 sera were found to contain antibodies that reacted with 5–20 discrete dots in the cell cytoplasm. Human antibodies colocalized with rabbit anti-DCP1a antibodies, confirming that these sera contained anti-

P-body antibodies (Bloch et al. 2005; Yu et al. 2005; Yang et al. 2006). Seven of the 34 human sera were used in this study to screen a protein macroarray prepared from phytohemagglutinin-treated human T-lymphocytes. The macroarray consists of a membrane with a 48-by-48 pattern of blocks. Each of the blocks contains 25 squares and 12 proteins are present, in duplicate, surrounding a central ink spot (see Fig. 1). The array contains ~17,000 proteins. A total of 67 immunoreactive proteins were identified (Table 1). These proteins included four known P-body components, DCP1a, TTP, Ge-1, and RAP55 (van Dijk et al. 2002; Fenger-Gron et al. 2005; Yu et al. 2005; Anderson and Kedersha 2006; Yang et al. 2006). In addition to Ge-1 and RAP55, three other PBC autoantigens, E3 pyruvate dehydrogenase complex, lamin A/C, and valosin-containing protein, were identified (Courvalin and Worman 1997; Palmer et al. 1999; Miyachi et al. 2004). Some of the sera reacted with autoantigens that are not usually associated with PBC, including CALR, GRIPAP1, SART1, and U1A (Bringmann et al. 1983; McCauliffe et al. 1990; Shichijo et al. 1998; Stinton et al. 2005). The remaining antigens, arranged in Table 1 using the Gene Ontology Consortium annotation system (Ashburner et al. 2000), include RNA-binding proteins, kinases and phosphatases, proteins involved in protein biosynthesis, and miscellaneous proteins. Thirteen additional antigens, not listed in Table 1, include unidentified proteins ( $n = 5$ ) and uncharacterized, potential open reading frames ( $n = 8$ ). Y-box protein 1 (YB-1) was chosen for further investigation because it

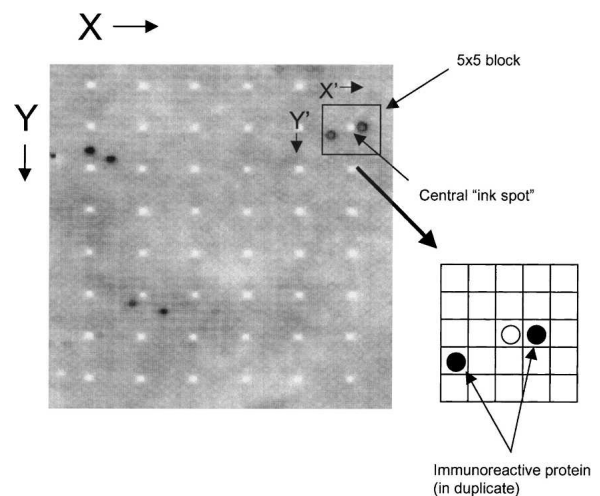


**FIGURE 1.** Antibodies in the serum of primary biliary cirrhosis patients react with proteins on a macroarray. The macroarray consists of 2304 blocks arranged in a 48-by-48 array. Each block consists of 24 squares surrounding a central ink spot. Twelve proteins are present, in duplicate, in each block. A section of the film produced by probing the macroarray with serum from a patient with PBC is shown. Detection of an immunoreactive protein requires the presence of two positive spots within a block, as indicated. The coordinates of an immunoreactive protein are determined by the X and Y axes of the blocks and the  $x'$  and  $y'$  axes of the positive dots within each block.

**TABLE 1.** Proteins identified on a macroarray using human sera containing anti-P-body autoantibodies

| Accession #  | Category/protein     | Patient |     |     |     |     |     |     |
|--------------|----------------------|---------|-----|-----|-----|-----|-----|-----|
|              |                      | Ge      | 004 | 017 | 038 | 061 | 080 | 121 |
|              | P-body components    |         |     |     |     |     |     |     |
| NM_018403    | DCP1a                | N       | P   | N   | N   | N   | N   | N   |
| NM_014329    | Ge-1/HEDLS/EDC4      | P       | P   | P   | N   | N   | N   | P   |
| NM_015578    | RAP55                | P       | P   | N   | P   | N   | P   | N   |
| NM_003407    | TTP/ZFP36            | P       | N   | N   | N   | N   | N   | N   |
| NM_004559    | YB1                  | N       | P   | P   | P   | N   | P   | N   |
|              | PBC autoantigens     |         |     |     |     |     |     |     |
| NM_000108    | E3 PDC/DLD           | P       | P   | P   | N   | N   | N   | P   |
| NM_170708    | LMNA                 | N       | P   | P   | N   | P   | P   | N   |
| NM_004559    | VCP                  | N       | P   | P   | N   | P   | P   | P   |
|              | Other autoantigens   |         |     |     |     |     |     |     |
| NM_004343    | CALR                 | N       | N   | N   | N   | N   | N   | P   |
| NM_020137    | GRIPAP1              | P       | P   | P   | P   | P   | P   | P   |
| NM_005146    | SART1                | P       | P   | N   | P   | P   | P   | P   |
| NM_004596    | U1A                  | P       | N   | P   | P   | P   | P   | P   |
|              | RNA-binding          |         |     |     |     |     |     |     |
| NM_007158    | CSDE1                | N       | N   | N   | N   | N   | P   | P   |
| NM_015033    | FNBP1                | N       | P   | N   | N   | N   | N   | N   |
| NM_004960    | FUS                  | P       | N   | N   | N   | N   | N   | N   |
| NM_031372    | HNRPDL               | N       | P   | N   | N   | P   | N   | P   |
| NM_031266    | HNRPAB               | P       | P   | P   | P   | P   | P   | P   |
| NM_004501    | HNRPU                | N       | P   | N   | P   | P   | N   | P   |
| NM_005792    | MPHOSPH6             | P       | P   | P   | P   | N   | P   | P   |
| NM_017948    | NOL8                 | N       | N   | N   | P   | N   | P   | N   |
| NM_002819    | PTPB1                | P       | P   | P   | P   | P   | P   | P   |
| NM_006753    | SURF6                | P       | P   | P   | P   | P   | P   | N   |
|              | Protein biosynthesis |         |     |     |     |     |     |     |
| NM_001961    | EEF2                 | P       | P   | P   | P   | P   | P   | P   |
| NM_015904    | EIF5B                | P       | P   | P   | P   | P   | P   | P   |
|              | Helicase             |         |     |     |     |     |     |     |
| NM_175066    | DDX51                | P       | P   | P   | P   | P   | P   | P   |
| NM_018183    | SBNO1                | N       | N   | P   | N   | N   | N   | N   |
|              | Kinase/phosphatase   |         |     |     |     |     |     |     |
| NM_004418    | DUSP2                | N       | P   | P   | P   | P   | N   | P   |
| NM_014330    | PPP1R15A             | N       | N   | N   | P   | N   | N   | N   |
| NM_006244    | PPP2R5B              | N       | P   | N   | N   | N   | N   | N   |
| NM_002719    | PPP2R5C              | N       | P   | P   | P   | P   | P   | N   |
| NM_005026    | PIK3CD               | N       | P   | N   | N   | N   | P   | N   |
| NM_002831    | PTPN6                | N       | N   | P   | N   | N   | N   | N   |
|              | Transcription        |         |     |     |     |     |     |     |
| NM_012138    | AATF                 | P       | P   | P   | N   | P   | P   | P   |
| NM_003655    | CBX4                 | P       | P   | P   | P   | P   | P   | P   |
| NM_022466    | IKZF5                | N       | P   | P   | P   | P   | P   | P   |
| NM_002360    | MAFK                 | P       | P   | P   | P   | P   | P   | P   |
| NM_003926    | MBD3                 | N       | P   | P   | P   | P   | N   | P   |
| NM_001040443 | PHF11                | P       | N   | N   | N   | N   | N   | N   |
| NM_002624    | PFDN5                | N       | P   | N   | N   | N   | N   | N   |
| NM_021975    | RELA                 | N       | P   | P   | P   | P   | P   | P   |
| NM_013376    | SERTAD1              | P       | P   | P   | N   | N   | P   | P   |
| NM_003086    | SNAPC4               | N       | N   | N   | P   | P   | N   | P   |
| NM_024061    | ZNF655               | N       | N   | N   | N   | N   | N   | P   |

(continued)

TABLE 1. Continued

| Accession #  | Category/protein | Patient |     |     |     |     |     |     |
|--------------|------------------|---------|-----|-----|-----|-----|-----|-----|
|              |                  | Ge      | 004 | 017 | 038 | 061 | 080 | 121 |
|              | Miscellaneous    |         |     |     |     |     |     |     |
| NM_006796    | AFG3L2           | N       | P   | P   | N   | N   | N   | N   |
| NM_004886    | APBA3            | P       | P   | P   | P   | P   | P   | N   |
| NM_018690    | APOB48R          | P       | P   | P   | P   | P   | P   | P   |
| NM_00333     | ATXN7            | N       | P   | P   | N   | N   | N   | N   |
| NM_004281    | BAG3             | N       | P   | N   | N   | N   | N   | N   |
| NM_001919    | DCI              | N       | N   | N   | P   | N   | N   | N   |
| NM_004082    | DCTN1            | N       | P   | P   | N   | P   | N   | N   |
| NM_024329    | EFHD2            | N       | P   | N   | N   | N   | N   | N   |
| NM_002569    | FURIN            | P       | N   | N   | P   | N   | N   | N   |
| NM_015710    | GLTSCR2          | P       | P   | N   | P   | P   | N   | N   |
| NM_000852    | GSTP1            | N       | P   | N   | N   | N   | N   | N   |
| NM_002117    | HLA-C            | P       | P   | P   | P   | P   | P   | P   |
| NM_015190    | HSP40            | P       | P   | P   | P   | P   | P   | P   |
| NM_021070    | LTBP3            | P       | P   | P   | P   | P   | P   | P   |
| NM_002473    | MYH9             | N       | P   | P   | P   | P   | P   | P   |
| NM_007346    | OGFR             | N       | N   | P   | N   | N   | N   | N   |
| NM_194248    | OTOF             | N       | N   | P   | N   | N   | N   | N   |
| NM_017884    | PINX1            | P       | N   | N   | N   | N   | N   | N   |
| NM_017647    | FTSJ3            | P       | P   | P   | P   | N   | P   | P   |
| NM_003612    | SEMA7A           | N       | P   | P   | P   | P   | N   | P   |
| NM_005412    | SHMT2            | P       | N   | N   | N   | N   | N   | N   |
| NM_014350    | TNFAIP8          | N       | P   | P   | N   | P   | N   | P   |
| NM_000391    | TPP1             | N       | N   | P   | N   | N   | P   | N   |
| NM_001008563 | USP20            | N       | P   | P   | P   | P   | P   | P   |

Abbreviations: P, immunoreactive; N, nonreactive.

contains RNA-binding domains and because it was previously shown to have a role in regulating mRNA stability (Evdokimova et al. 2001; Nekrasov et al. 2003).

### Y-box protein 1 is a component of mRNA processing bodies

YB-1 is a 50-kDa protein that is the predominant component of translationally inactive mRNA-ribonucleoprotein particles (Minich et al. 1989; Evdokimova et al. 1995). YB-1 stabilizes mRNAs that have a 5' cap but lack the eIF4e cap-binding protein (Evdokimova et al. 2001; Nekrasov et al. 2003). YB-1 may protect message from degradation until readdition of eIF4e and return of the mRNA to active translation in polysomes. Overexpression of YB-1 represses mRNA translation and increases mRNA stability. Depletion of YB-1 results in accelerated mRNA decay (Evdokimova et al. 2001).

YB-1 consists of an alanine- and proline-rich N-terminal domain (amino acids 1–55), followed by a cold shock domain (56–128) and a C-terminal region that contains four clusters of basic and acidic amino acids (129–324) (for review, see Kohno et al. 2003). The cold shock domain binds to both DNA and RNA. The C terminus of YB-1 also binds DNA and RNA and mediates protein–protein interactions. The functions of the YB-1 N terminus are unknown.

To investigate the cellular location of YB-1, a plasmid encoding green fluorescent protein (GFP) fused to the N terminus of YB-1 was transfected into Hep-2 cells. In cells expressing GFP–YB-1, antibodies directed against GFP localized to cytoplasmic dots and colocalized with antibodies directed against DCP1a (Fig. 2, panels a–c). To consider the possibility that GFP contributed to the localization of YB-1 to P-bodies, a plasmid encoding FLAG epitope fused to YB-1 was prepared and transfected into cells. FLAG–YB-1 was also detected in mRNA P-bodies (Fig. 2, panels d–f). To demonstrate that endogenous YB-1 also localizes to P-bodies, cells were stained with rabbit anti-YB-1 antiserum and human serum 121. As determined using the protein macroarray, this human serum reacted with Ge-1, but not YB-1. In addition to staining mRNA P-bodies, serum 121 also stained 5–20 dots in the nucleus of Hep-2 cells, reflecting the presence of autoantibodies directed against promyelocytic leukemia (PML) nuclear bodies (Fig. 2, panel h). Rabbit anti-YB-1 antiserum stained P-bodies but did not react with PML nuclear bodies (Fig. 2, panel g). Taken together, these results indicate that endogenous YB-1 is a component of P-bodies.

To identify the portion of YB-1 that directs the protein to P-bodies, expression vectors encoding GFP fused to various segments of YB-1 were transfected into Hep-2 cells. Results are summarized in Figure 3A, and representative

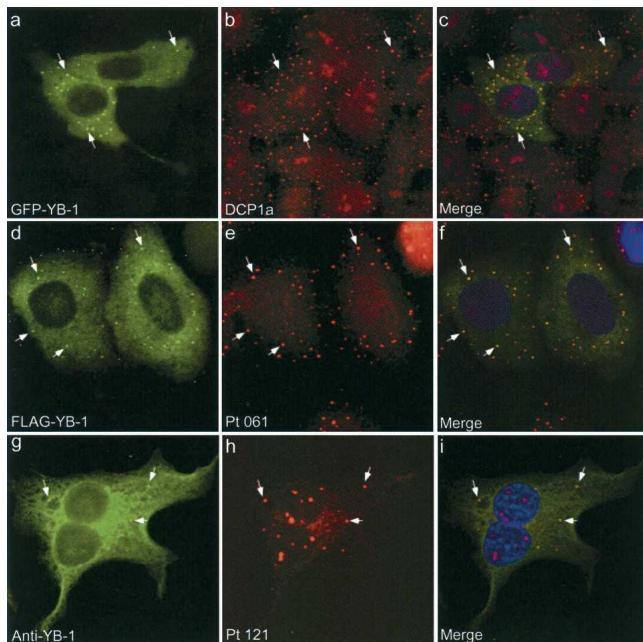


**FIGURE 2.** YB-1 localizes to mRNA processing bodies. Indirect immunofluorescence was used to show that YB-1 localizes to P-bodies. GFP-YB-1 (green, panel a) localized to discrete, dot-like structures in the cytoplasm of transfected Hep-2 cells and colocalized with P-bodies recognized by rabbit anti-DCP1a antiserum (red, panel b). FLAG-YB-1 also localized to cytoplasmic dots (green, panel d) and colocalized with P-bodies identified using serum from patient 061 (red, panel e). To determine whether endogenous YB-1 also localized to P-bodies, rabbit anti-YB-1 antiserum (green, panel g) and human serum 121 (red, panel h) were used to stain Hep-2 cells. Serum 121 reacted with both P-bodies and PML nuclear bodies. In contrast, rabbit anti-YB-1 antiserum detected YB-1 within P-bodies and diffusely throughout the cytoplasm, but did not stain PML-nuclear bodies. White arrows indicate the location of representative P-bodies in transfected cells. DAPI staining (blue) indicates the location of nuclei. Overlap of red, green, and blue staining is shown in panels c, f, and i.

photomicrographs are shown in Figure 3B. Successful production of GFP-YB-1 fusion proteins was confirmed by immunoblot using rabbit anti-GFP antiserum (data not shown). A GFP fusion protein containing YB-1 amino acids 1–281 localized to P-bodies, showing that the C-terminal 43 amino acids were not required for P-body localization (Fig. 3B, panels a–c). N-terminal (1–205) and C-terminal (128–324) segments of YB-1 were detected in nuclei and nucleoli and did not localize to P-bodies (Fig. 3B, panels d–i). Jurkott and colleagues and Bader and Vogt observed similar staining patterns using N- and C-terminal fragments of YB-1 (Jurkott et al. 2003; Bader and Vogt 2005). A portion of YB-1 (55–324) that lacked the N-terminal domain was present throughout transfected cells and was not concentrated in P-bodies (data not shown). These results indicate that the alanine-proline-rich N terminus, the cold shock domain, and amino acids 205–281 of the C terminus are required for P-body localization.

### YB-1 localizes to TIA-containing stress granules

To investigate the cellular location of YB-1 in response to environmental stress, GFP-YB-1 was transfected into Hep-2 cells and the cells were exposed to arsenite for 1 h. Under these conditions, YB-1 colocalized with TIA in stress granules (Fig. 4A, panels a–c). Stress granules appeared larger and more numerous in YB-1 transfected cells, suggesting that YB-1 may contribute to stress granule formation and/or increase the stability of these structures. However, in control Hep-2 cells, expression of YB-1 did not alter the nuclear location of TIA, suggesting that YB-1 did not induce stress granule formation in the absence of oxidative stress (Fig. 4A, panels d–f). Note that endogenous YB-1, identified using rabbit anti-YB-1 antiserum, also localized to stress granules in response to oxidative stress (Fig. 4A, panels g–i).

To identify the portion of YB-1 that is required for localization to stress granules, Hep-2 cells were transfected with plasmids encoding GFP fused to DNA encoding portions of the protein. Although a fusion protein (GFP-YB-1 [55–324]) that lacked the YB-1 N-terminal domain was unable to localize to P-bodies, this fusion protein was capable of localizing to stress granules (Fig. 4B, panels a–c). In contrast, a fusion protein (GFP-YB-1 [128–324]) that lacked both the N-terminal domain and the cold shock domain did not associate with stress granules (Fig. 4B, panels d–f). A fusion protein (GFP-YB-1 [1–205]) that contained the N-terminal and cold shock domains localized to stress granules, but a fusion protein (GFP-YB-1 [1–86]) that lacked the C-terminal 42 amino acids of the cold shock domain did not localize to these structures (data not shown). A small segment of YB-1 (amino acids 44–128), containing the cold shock domain, was sufficient to direct GFP to stress granules (Fig. 4B, panels g–i). These results indicate that neither the N-terminal nor the C-terminal domain of YB-1 was required for stress granule localization.

In a previous study, we showed that P-body component RAP55, like YB-1, is capable of translocating from P-bodies to stress granules (Yang et al. 2006). To examine the cellular location of YB-1 compared to that of RAP55 during arsenite-induced stress, cells were transfected with plasmids encoding FLAG-YB-1 and GFP-RAP55 and were exposed to arsenite. Both YB-1 and RAP55 were detected in stress granules (Fig. 4C, panels a–c). To determine the cellular location of YB-1 during recovery from stress, YB-1- and RAP55-transfected cells were exposed to arsenite for 1 h, rinsed with PBS, and then permitted to recover in culture medium for 1, 3, 5, or 12 h. One hour after removal of arsenite, RAP55 was detected both within stress granules and in adjacent P-bodies (Fig. 4C, panel d). In contrast, YB-1 persisted in stress granules (Fig. 4C, panel e). After 3 h of recovery from stress, RAP55 was detected within P-bodies but was no longer present in stress granules. YB-1 remained in stress granules or was distributed diffusely throughout the cytoplasm, but was not detected

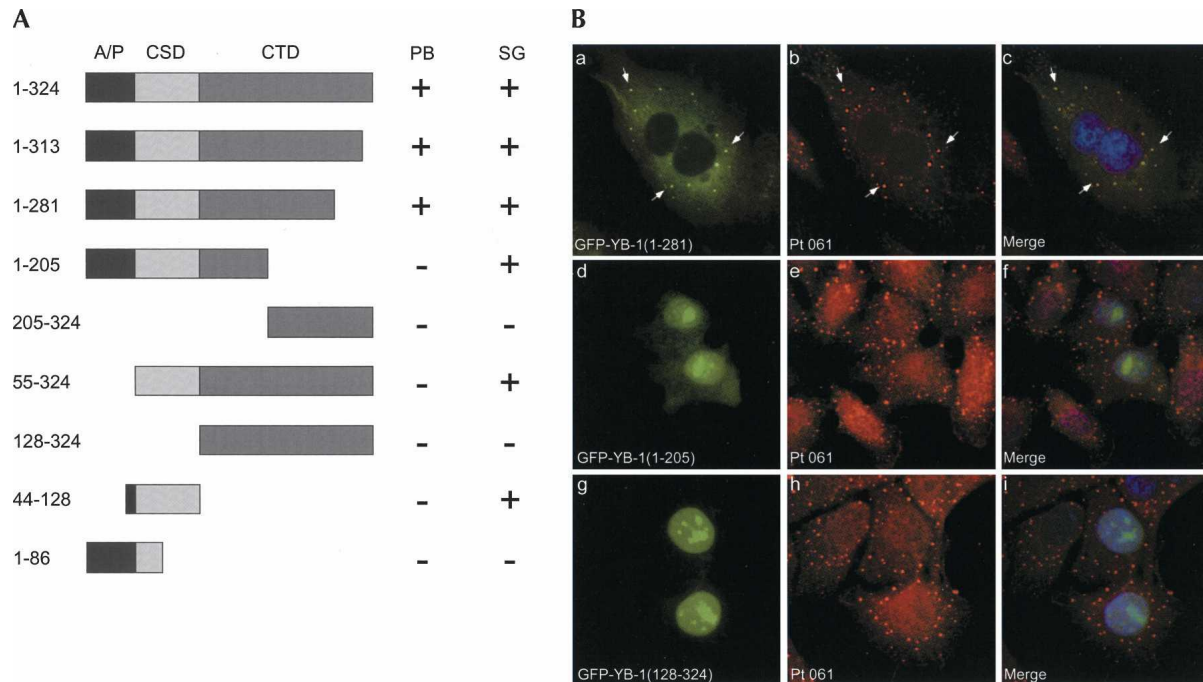


**FIGURE 3.** Structure of YB-1 and identification of the portions of YB-1 that mediate localization to P-bodies. (A) The predicted amino acid sequence of YB-1 contains an N-terminal alanine-proline rich region (A/P) and a cold shock domain (CSD). The C-terminal domain (CTD) contains alternating basic and acidic segments. The portions of YB-1 that were capable of localizing green fluorescent protein (GFP) to P-bodies (PB) or stress granules (SG) are indicated by “+.” Representative indirect immunofluorescence results are shown in B. (B) Indirect immunofluorescence was used to identify the portion of YB-1 that was necessary for localization to P-bodies. A segment of YB-1 containing amino acids 1–281 (green, panel a) colocalized with P-bodies that were identified using serum from patient 061 (red, panel b). White arrows indicate representative P-bodies. N-terminal (1–205) and C-terminal (128–324) portions of YB-1 localized to nuclei and nucleoli (green, panels d and g) but did not localize to P-bodies (red, panels e and h). DAPI staining (blue) indicates the location of nuclei. Merge of red, green, and blue staining is shown in panels c, f, and i.

in P-bodies (data not shown). At 5 and 12 h after removal of arsenite, both RAP55 and YB-1 were detected in P-bodies (data not shown). The differing cellular location of RAP55 and YB-1 during the early stages of recovery from stress suggests that these proteins may have different roles in the “sorting” of mRNAs that occurs in stress granules. RAP55 may escort some mRNAs from stress granules to P-bodies. In contrast, YB-1 may transfer other mRNAs from stress granules back to polyribosomes.

## Conclusions

In this study, we used protein macroarray technology and human autoantibodies to identify four known, and 63 potential, components of mRNA P-bodies. The possible relationship between the majority of these antigens and P-bodies remains to be determined. We showed that one of these proteins, YB-1, does localize to P-bodies. The alanine-proline-rich N terminus, the cold shock domain, and the N-terminal half of the C-terminal domain were required to target YB-1 to P-bodies. A much smaller portion of the protein, which contained the cold shock domain, was necessary and sufficient to target the protein to stress granules. YB-1 is similar to RAP55 in that it translocates to stress granules in response to oxidative stress. In contrast to RAP55, YB-1

does not return to P-bodies during the immediate recovery period.

YB-1 protects mRNA from degradation and is particularly effective at mRNA stabilization when it binds, in the absence of eIF4e, to the 5' cap. We speculate that the role of YB-1 in P-bodies may be to protect mRNA from degradation, possibly allowing readdition of eIF4e and return of the mRNA to polysomes. Consistent with this model, YB-1 may be excluded from P-bodies during recovery from stress because, during this critical period, P-bodies are actively involved in the destruction of damaged mRNA.

This is the first study to use protein macroarrays and human autoantibodies to define the composition of a cellular structure. We anticipate that the combination of macroarrays and autoantibodies will prove to be an efficient approach to identifying additional components of P-bodies and that “autoantigenomics” may be applied to the study of other cellular domains.

## MATERIALS AND METHODS

### Plasmids and antisera

A plasmid encoding YB-1 was obtained from the German Resource Center for Genome Research (RZPD, Berlin, Germany;

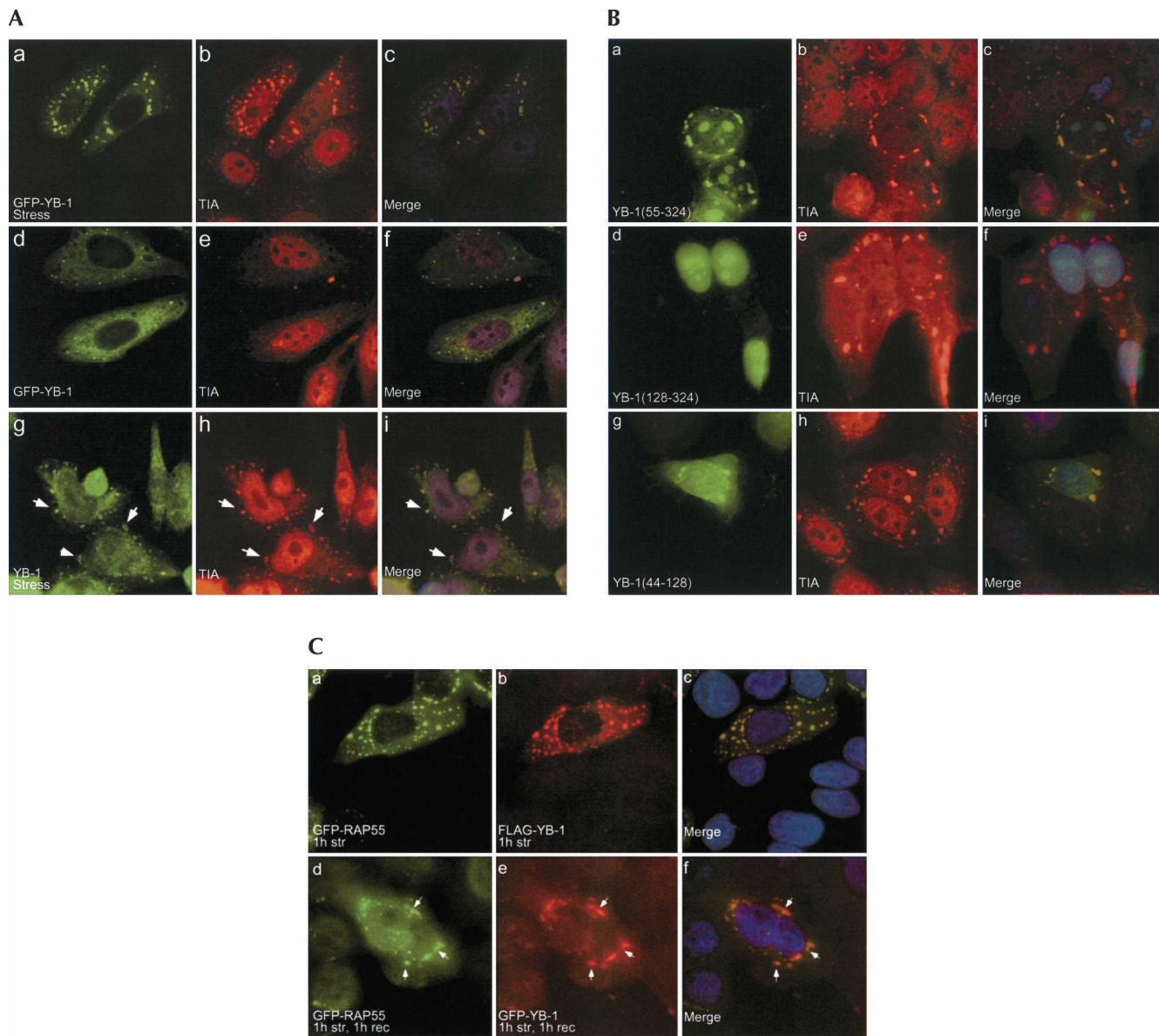


**FIGURE 4.** YB-1 localizes to stress granules. (A) A plasmid encoding GFP–YB-1 was transfected into Hep-2 cells and cells were exposed to arsenite for 1 h. In transfected cells, GFP–YB-1 (green, panel a) colocalized with TIA (red, panel b) in stress granules. In control cells, expression of GFP–YB-1 (green, panel d) did not induce stress granule formation (red, panel e). Endogenous YB-1 (green, panel g) also localized to stress granules (red, panel h) in response to oxidative stress. White arrows in panels g–i indicate the location of representative stress granules. DAPI staining (blue) indicates the location of nuclei. Merge of red, green, and blue is shown in panels c, f, and i. (B) A fusion protein (GFP–YB-1 [55–324]) that lacked the N-terminal domain of YB-1 (green, panel a) localized to stress granules (red, panel b). A fusion protein (GFP–YB-1 [128–324]) that lacked both the N-terminal domain and the cold shock domain (green, panel d) did not localize to stress granules (red, panel e). A fragment of YB-1 that contained the cold shock domain (44–128) (green, panel g) was sufficient to direct GFP to stress granules (red, panel h). DAPI staining (blue) indicates the location of nuclei. Merge of red, green, and blue staining is shown in panels c, f, and i. (C) To examine the cellular location of YB-1 compared to that of RAP55 during arsenite-induced stress, cells were cotransfected with GFP–RAP55 (green, panel a) and FLAG–YB-1 (red, panel b) and exposed to arsenite. Both YB-1 and RAP55 were detected in stress granules. In cells exposed to arsenite and then permitted to recover for 1 h, RAP55 was detected within stress granules and within adjacent P-bodies (green, panel d). In contrast, YB-1 (red, panel e) persisted in stress granules. White arrows in panels d–f indicate the presence of P-bodies (panels d and f) or absence of P-bodies (panel e) adjacent to stress granules. DAPI staining (blue) indicates the location of nuclei. Merge of red, green, and blue staining is shown in panels c and f.

catalogue number: RZPDp9016E0814). The cDNA was ligated into pEGFP (Clontech) and pCMV-FLAG (Invitrogen) to produce green fluorescence protein (GFP)–YB-1 and FLAG–YB-1 fusion proteins, respectively. Plasmids encoding GFP fused to amino

acids 1–313, 1–281, 1–205, and 1–86 were prepared using YB-1 cDNA restriction sites *EcoRI*, *KpnI*, *SalI*, and *BsrGI*, respectively. A plasmid encoding YB-1 amino acids 205–324 was prepared by ligating YB-1 cDNA *SalI* fragment into pEGFP. PCR was used to

prepare DNA encoding YB-1 amino acids 55–324, 128–324, and 44–128. The nucleotide sequence of each PCR product was confirmed by DNA sequencing. A plasmid encoding GFP fused to RAP55 was previously described (Yang et al. 2006).

Sera from 34 patients with anti-P-body antibodies were identified during the course of studies to determine the clinical significance of autoantibodies in patients with PBC (Yang et al. 2004). Ge serum and patient sera 080 and 017 were previously used to identify and characterize P-body components Ge-1 and RAP55 (Yu et al. 2005; Yang et al. 2006). The remaining four sera (004, 038, 061, and 121) produced a typical P-body staining pattern. Two of the seven patient sera (Ge and 121) reacted with PML nuclear bodies, as well as P-bodies.

Rabbit anti-DCP1a and anti-YB-1 antisera were provided by J. Lykke-Andersen (University of Colorado, Boulder, CO) and P.E. Newburger (University of Massachusetts, Worcester, MA), respectively. Mouse and rabbit anti-GFP antisera were obtained from Invitrogen. Mouse anti-FLAG antiserum was purchased from Sigma-Aldrich. Goat anti-TIA antiserum was obtained from Santa Cruz Biotechnology. FITC- or rhodamine-conjugated, species-specific, donkey anti-human, anti-goat, anti-rabbit, and anti-mouse IgG antisera were obtained from Jackson ImmunoResearch Laboratories.

### Cell culture and immunohistochemistry

Hep-2 cells were obtained from ATCC and maintained in DMEM supplemented with 10% Nuserum (BD Bioscience), L-glutamine (2 mM), penicillin (200 U/mL), and streptomycin (200 µg/mL). For immunofluorescent staining, Hep-2 cells were grown in tissue culture chambers (Nunc Inc.), fixed with 2% paraformaldehyde in PBS, and permeabilized with 100% methanol. Cells were stained with primary and secondary antisera as previously described (Bloch et al. 2005).

### Screening the high-density protein macroarray

High-density protein macroarrays derived from human T-cells treated with PHA were obtained from RZPD. Membranes were initially rinsed in 100% ethanol at room temperature, incubated in blocking solution (3% nonfat, dry milk powder in TBST [TBS, 0.1% v/v Tween 20]) for 2 h and washed twice in TBST. Membranes were then incubated overnight at 4°C with human serum diluted 1:3000 in blocking solution. Bound antibodies were detected using horse-radish peroxidase-conjugated rabbit anti-human IgG antiserum (Sigma-Aldrich) and chemiluminescence.

### Mammalian cell transfection

To identify the portion of YB-1 that mediates localization to P-bodies, plasmids encoding GFP fused to segments of YB-1 were transfected into Hep-2 cells using the Effectene transfection system (Qiagen) as directed by the manufacturer. Cells were fixed and stained 24 h after transfection. To identify the portion of YB-1 that mediates stress granule localization, transfected cells were exposed to sodium arsenite (0.5 mM) for 1 h at 37°C. To determine the cellular location of YB-1 during recovery from stress, arsenite-containing medium was removed and cells were washed with PBS and incubated in culture medium. Cells were permitted to recover for 1, 3, 5, and 12 h.

### ACKNOWLEDGMENTS

We thank J. Lykke-Andersen and P.E. Newburger for providing rabbit anti-DCP1a and anti-YB-1 antisera, respectively. S. Hennig (RZPD, Deutsches Ressourcenzentrum für Genomforschung, Berlin, Germany) assisted in the identification of proteins on the macroarrays. D.B.B. was supported by grants from the Arthritis Foundation, the Milton Fund, and the National Institutes of Health (DK051179).

Received November 29, 2006; accepted February 2, 2007.

### REFERENCES

- Anderson, P. and Kedersha, N. 2006. RNA granules. *J. Cell Biol.* **172**: 803–808.
- Ashburner, M., Ball, C.A., Blake, J.A., Botstein, D., Butler, H., Cherry, J.M., Davis, A.P., Dolinski, K., Dwight, S.S., Eppig, J.T., et al. 2000. Gene ontology: Tool for the unification of biology. The Gene Ontology Consortium. *Nat. Genet.* **25**: 25–29.
- Bader, A.G. and Vogt, P.K. 2005. Inhibition of protein synthesis by Y box-binding protein 1 blocks oncogenic cell transformation. *Mol. Cell. Biol.* **25**: 2095–2106.
- Bloch, D.B., Yu, J.H., Yang, W.H., Graeme-Cook, F., Lindor, K.D., Viswanathan, A., Bloch, K.D., and Nakajima, A. 2005. The cytoplasmic dot staining pattern is detected in a subgroup of patients with primary biliary cirrhosis. *J. Rheumatol.* **32**: 477–483.
- Bouveret, E., Rigaut, G., Shevchenko, A., Wilm, M., and Seraphin, B. 2000. A Sm-like protein complex that participates in mRNA degradation. *EMBO J.* **19**: 1661–1671.
- Bregues, M., Teixeira, D., and Parker, R. 2005. Movement of eukaryotic mRNAs between polyosomes and cytoplasmic processing bodies. *Science* **310**: 486–489.
- Bringmann, P., Rinke, J., Appel, B., Reuter, R., and Luhrmann, R. 1983. Purification of snRNPs U1, U2, U4, U5, and U6 with 2,2,7-trimethylguanosine-specific antibody and definition of their constituent proteins reacting with anti-Sm and anti-(U1)RNP antisera. *EMBO J.* **2**: 1129–1135.
- Bussow, K., Nordhoff, E., Lubbert, C., Lehrach, H., and Walter, G. 2000. A human cDNA library for high-throughput protein expression screening. *Genomics* **65**: 1–8.
- Coller, J.M., Tucker, M., Sheth, U., Valencia-Sanchez, M.A., and Parker, R. 2001. The DEAD box helicase, Dhh1p, functions in mRNA decapping and interacts with both the decapping and deadenylase complexes. *RNA* **7**: 1717–1727.
- Cougot, N., Babajko, S., and Seraphin, B. 2004. Cytoplasmic foci are sites of mRNA decay in human cells. *J. Cell Biol.* **165**: 31–40.
- Courvalin, J.C. and Worman, H.J. 1997. Nuclear envelope protein autoantibodies in primary biliary cirrhosis. *Semin. Liver Dis.* **17**: 79–90.
- Evdokimova, V.M., Wei, C.L., Sitikov, A.S., Simonenko, P.N., Lazarev, O.A., Vasilenko, K.S., Ustinov, V.A., Hershey, J.W., and Ovchinnikov, L.P. 1995. The major protein of messenger ribonucleoprotein particles in somatic cells is a member of the Y-box binding transcription factor family. *J. Biol. Chem.* **270**: 3186–3192.
- Evdokimova, V., Ruzanov, P., Imataka, H., Raught, B., Svitkin, Y., Ovchinnikov, L.P., and Sonenberg, N. 2001. The major mRNA-associated protein YB-1 is a potent 5' cap-dependent mRNA stabilizer. *EMBO J.* **20**: 5491–5502.
- Eystathioy, T., Jakymiw, A., Chan, E.K., Seraphin, B., Cougot, N., and Fritzler, M.J. 2003. The GW182 protein colocalizes with mRNA degradation associated proteins hDcp1 and hLSm4 in cytoplasmic GW bodies. *RNA* **9**: 1171–1173.
- Fenger-Gron, M., Fillman, C., Norrild, B., and Lykke-Andersen, J. 2005. Multiple processing body factors and the ARE binding protein TTP activate mRNA decapping. *Mol. Cell* **20**: 905–915.



- Horn, S., Lueking, A., Murphy, D., Staudt, A., Gutjahr, C., Schulte, K., Konig, A., Landsberger, M., Lehrach, H., Felix, S.B., et al. 2006. Profiling humoral autoimmune repertoire of dilated cardiomyopathy (DCM) patients and development of a disease-associated protein chip. *Proteomics* **6**: 605–613.
- Jakymiw, A., Lian, S., Eystathioy, T., Li, S., Satoh, M., Hamel, J.C., Fritzler, M.J., and Chan, E.K. 2005. Disruption of GW bodies impairs mammalian RNA interference. *Nat. Cell Biol.* **7**: 1167–1174.
- Jurchott, K., Bergmann, S., Stein, U., Walther, W., Janz, M., Manni, I., Piaggio, G., Fietze, E., Dietel, M., and Royer, H.D. 2003. YB-1 as a cell cycle-regulated transcription factor facilitating cyclin A and cyclin B1 gene expression. *J. Biol. Chem.* **278**: 27988–27996.
- Kaplan, M.M. and Gershwin, M.E. 2005. Primary biliary cirrhosis. *N. Engl. J. Med.* **353**: 1261–1273.
- Kedersha, N. and Anderson, P. 2002. Stress granules: Sites of mRNA triage that regulate mRNA stability and translatability. *Biochem. Soc. Trans.* **30**: 963–969.
- Kedersha, N., Stoecklin, G., Ayodele, M., Yacono, P., Lykke-Andersen, J., Fitzler, M.J., Scheuner, D., Kaufman, R.J., Golan, D.E., and Anderson, P. 2005. Stress granules and processing bodies are dynamically linked sites of mRNP remodeling. *J. Cell Biol.* **169**: 871–884.
- Kohno, K., Izumi, H., Uchiumi, T., Ashizuka, M., and Kuwano, M. 2003. The pleiotropic functions of the Y-box-binding protein, YB-1. *Bioessays* **25**: 691–698.
- Liu, J., Rivas, F.V., Wohlschlegel, J., Yates, J.R., Parker, R., and Hannon, G.J. 2005. A role for the P-body component GW182 in microRNA function. *Nat. Cell Biol.* **7**: 1161–1166.
- Lueking, A., Huber, O., Wirths, C., Schulte, K., Stieler, K.M., Blume-Peytavi, U., Kowald, A., Hensel-Wiegel, K., Tauber, R., Lehrach, H., et al. 2005. Profiling of alopecia areata autoantigens based on protein microarray technology. *Mol. Cell. Proteomics* **4**: 1382–1390.
- McCauliffe, D.P., Zappi, E., Lieu, T.S., Michalak, M., Sontheimer, R.D., and Capra, J.D. 1990. A human Ro/SS-A autoantigen is the homologue of calreticulin and is highly homologous with onchocercal RAL-1 antigen and an aplasia “memory molecule”. *J. Clin. Invest.* **86**: 332–335.
- Minich, W.B., Korneyeva, N.L., and Ovchinnikov, L.P. 1989. Translational active mRNPs from rabbit reticulocytes are qualitatively different from free mRNA in their translatability in cell-free system. *FEBS Lett.* **257**: 257–259.
- Miyachi, K., Hirano, Y., Horigome, T., Mimori, T., Miyakawa, H., Onozuka, Y., Shibata, M., Hirakata, M., Suwa, A., Hosaka, H., et al. 2004. Autoantibodies from primary biliary cirrhosis patients with anti-p95c antibodies bind to recombinant p97/VCP and inhibit in vitro nuclear envelope assembly. *Clin. Exp. Immunol.* **136**: 568–573.
- Nekrasov, M.P., Ivshina, M.P., Chernov, K.G., Kovrigina, E.A., Evdokimova, V.M., Thomas, A.A., Hershey, J.W., and Ovchinnikov, L.P. 2003. The mRNA-binding protein YB-1 (p50) prevents association of the eukaryotic initiation factor eIF4G with mRNA and inhibits protein synthesis at the initiation stage. *J. Biol. Chem.* **278**: 13936–13943.
- Palmer, J.M., Jones, D.E., Quinn, J., McHugh, A., and Yeaman, S.J. 1999. Characterization of the autoantibody responses to recombinant E3 binding protein (protein X) of pyruvate dehydrogenase in primary biliary cirrhosis. *Hepatology* **30**: 21–26.
- Sheth, U. and Parker, R. 2003. Decapping and decay of messenger RNA occur in cytoplasmic processing bodies. *Science* **300**: 805–808.
- Shichijo, S., Nakao, M., Imai, Y., Takasu, H., Kawamoto, M., Niiya, F., Yang, D., Toh, Y., Yamana, H., and Itoh, K. 1998. A gene encoding antigenic peptides of human squamous cell carcinoma recognized by cytotoxic T lymphocytes. *J. Exp. Med.* **187**: 277–288.
- Stinton, L.M., Selak, S., and Fritzler, M.J. 2005. Identification of GRASP-1 as a novel 97 kDa autoantigen localized to endosomes. *Clin. Immunol.* **116**: 108–117.
- van Dijk, E., Cougot, N., Meyer, S., Babajko, S., Wahle, E., and Seraphin, B. 2002. Human Dcp2: A catalytically active mRNA decapping enzyme located in specific cytoplasmic structures. *EMBO J.* **21**: 6915–6924.
- Yang, W.H., Yu, J.H., Nakajima, A., Neuberg, D., Lindor, K., and Bloch, D.B. 2004. Do antinuclear antibodies in primary biliary cirrhosis patients identify increased risk for liver failure? *Clin. Gastroenterol. Hepatol.* **2**: 1116–1122.
- Yang, W.H., Yu, J.H., Gulick, T., Bloch, K.D., and Bloch, D.B. 2006. RNA-associated protein 55 (RAP55) localizes to mRNA processing bodies and stress granules. *RNA* **12**: 547–554.
- Yu, J.H., Yang, W.H., Gulick, T., Bloch, K.D., and Bloch, D.B. 2005. Ge-1 is a central component of the mammalian cytoplasmic mRNA processing body. *RNA* **11**: 1795–1802.